Atomistic Simulation of Poly(dimethylsiloxane): Force Field Development, Structure, and Thermodynamic Properties of Polymer Melt and Solubility of *n*-Alkanes, *n*-Perfluoroalkanes, and Noble and Light Gases

Zoi A. Makrodimitri,[†] Ralf Dohrn,[‡] and Ioannis G. Economou*,[†]

Molecular Thermodynamics and Modeling of Materials Laboratory, Institute of Physical Chemistry, National Center of Scientific Research "Demokritos", GR-153 10 Aghia Paraskevi Attikis, Greece, and Bayer Technology Services GmbH, D-51368, Leverkusen, Germany

Received October 24, 2006; Revised Manuscript Received December 15, 2006

ABSTRACT: Poly(dimethylsiloxane) (PDMS) is a widely used polymer for a number of industrial applications. In order that PDMS is selected for a specific application, accurate knowledge of its physical properties is necessary. Physical properties can be either measured or calculated based on reliable suitable methods. Molecular simulation using realistic models is a powerful tool for the elucidation of microscopic structure of polymers and the subsequent estimation of macroscopic physical properties. In this work, a force field is developed for the prediction of thermodynamic and structure properties of PDMS melts. Force field development was based on existing force fields for PDMS together with fitting to experimental thermodynamic data at ambient pressure. Extensive *NPT* molecular dynamics (MD) simulations were performed at different temperature and pressure values. In all cases, good agreement was obtained between literature experimental data and model predictions for the melt density. Calculations are reported also for the solubility parameter of the polymer melt at different temperatures. Furthermore, radial distribution functions for the intra- and intermolecular interactions are presented and shown to be in good agreement with previous literature work. The new force field is used subsequently for the calculation of solubility of 17 different compounds in PDMS using the Widom test particle insertion method. The solubility of *n*-alkanes from methane to *n*-hexane at 300 and 450 K and different pressures was calculated. In addition, solubility calculations for *n*-perfluoroalkanes at 300 and 450 K and for noble and light gases at 300, 375, and 450 K and ambient pressure were performed. Model predictions are in very good agreement with experimental data, in all cases. The infinite dilution solubility coefficient is shown to increase with temperature for very light gases and decrease for the heavier ones.

1. Introduction

Silicon polymers, such as poly(dimethylsiloxane) (PDMS), are used extensively in many industrial applications including adhesives, coatings and elastomeric seals, due to their unique physical properties. PDMS has one of the lowest glass transition temperatures among known polymers and is stable at relatively high temperatures. These properties make it an interesting polymer both scientifically and commercially. For example, PDMS is the most commonly used membrane material for separation of organic vapors and gases.[1] PDMS is biocompatible and used for different medical purposes, e.g., for implants. In industrial polymer process design, PDMS is often used as a model substance, since it shows very similar relevant properties at ambient conditions as the industrial polymers at process conditions (up to 700 K). An improved understanding of mixtures of PDMS and volatile components, especially phase equilibria and diffusion coefficients, is important for the development of new techniques for polymer finish processing. These developments are triggered by permanently increasing demands for higher polymer quality, e.g., optical grade quality polycarbonate for high-density optical storage systems. Some major goals of polymer finish processing are the efficient removal of undesired impurities from the polymerization process like catalyst, monomer, oligomer and solvent molecules as well as (mostly) white color, homogeneity, and constant quality.[2]

The ability to predict the properties of polymeric materials based on their chemical structure is critical for the selection, improvement and design of polymer products in an industrial application. Considerable work has been performed on the correlation of PDMS *PVT* properties using equation-of-state theories.[3−5] Moreover, a wealth of experimental data have been reported on the solubility and diffusivity of light gases, *n*-alkanes, perfluoroalkanes and other compounds in PDMS at different temperatures and pressures.[6−19]

Accurate computational methods are an appealing alternative to experiments since they are less costly and time-consuming and provide greater flexibility in terms of conditions and/or components explored. The tremendous increase of computing power at relatively low price and advances in applied statistical mechanics in recent years have made molecular simulation a powerful tool for the elucidation of microscopic phenomena that control macroscopic properties for a wide range of complex materials, including fluid mixtures, polymers, solids, etc.[20,21] This has made possible the estimation of the thermodynamic properties of pure polymer melts as well as the calculation of solubility and diffusion coefficients of penetrants in polymers via molecular dynamic (MD) simulation techniques. Finally, molecular simulation allows the microscopic understanding of the permeation of molecules dissolved in dense polymers which is important in membrane processes and the development of barrier materials.

* Corresponding author: economou@chem.demokritos.gr.
[†] Molecular Thermodynamics and Modeling of Materials Laboratory, Institute of Physical Chemistry, National Center of Scientific Research "Demokritos".
[‡] Bayer Technology Services GmbH.

10.1021/ma062453f CCC: $37.00
Published on Web 02/09/2007

One of the first attempts to simulate PDMS at a molecular level was the work of Sok et al.[22] who developed a force field for the polymer and used it subsequently for the calculation of solubility and diffusion coefficient of helium and of methane in it at ambient conditions. Simulation results for the solubility coefficient deviated significantly from experimental data while good agreement was obtained for the case of diffusion coefficient. Subsequent MD simulations for other gases dissolved in PDMS verified the poor agreement between experiment and simulation for the case of solubility coefficient,[23] while simulations with a different force field verified the good agreement for the case of diffusion coefficient of gases in PDMS.[24] The permeation of polar mixtures in PDMS has been also investigated with MD.[25,26]

A refined force field for PDMS was developed by Curro and co-workers[27,28] and used for the calculation of microscopic structure of the polymer melt, again at ambient conditions. Good agreement between experiment and simulation was reported. Sun[29] developed an explicit atom force field (referred to as CFF) for PDMS based on quantum chemistry calculations on corresponding oligomers and used it for the prediction of thermodynamic, structural and vibrational properties of PDMS. Good agreement with experiment was observed in all cases. Recently, a slightly modified CFF force field was developed by Smith et al.[30] based on more complex oligomers of PDMS and at higher level of quantum chemistry calculations. Until now, however, no molecular simulations have been reported for the solubility and diffusion coefficient of larger *n*-alkanes in PDMS.

In this work, a united atom (UA) force-field is developed for the calculation of microscopic structure, thermodynamic and conformational properties of pure PDMS melts over a wide temperature and pressure range. The bonded, electrostatic and Lennard-Jones (LJ) parameters for Si and O proposed by Sok et al.[22] for PDMS are adopted, while CH_3 parameters are adjusted to match the experimental density of PDMS at ambient conditions. This force field is used subsequently to study PDMS melt properties at higher temperatures and pressures. Furthermore, the solubility coefficients of *n*-alkanes from methane to *n*-hexane, of *n*-perfuoroalkanes from perfluoromethane to *n*-perfluorobutane, of five noble gases (He, Ne, Ar, Kr and Xe) and of two light gases (N_2 and O_2) in PDMS are calculated. Appropriate atomistic force fields from the literature are used. Simulations are performed at 300 and 450 K and ambient pressure. For the case of *n*-alkanes, higher pressures are also examined, while for the gases solubility calculations are also performed at 375 K. In all cases where experimental data are available, good agreement between simulation and experiment is obtained.

2. Force Field Development

Poly(dimethylsiloxane) is a flexible polymer whose molecular architecture consists of an alternating silicon−oxygen backbone, with two methyl groups attached to every silicon atom, as shown schematically in Figure 1. Realistic atomistic force fields for macromolecules account explicitly for the molecular geometric characteristics as well as for the nonbonded intra- and intermolecular interactions.[31] In this work, a force field is developed for PDMS based on the united atom (UA) representation. In the UA representation, hydrogen atoms in the methyl groups are not accounted explicitly, thus reducing the number of "atoms" significantly. For PDMS, this approach reduces the number of "atoms" per monomer from ten to four. In the force field developed, the potential energy function is written as the sum of contributions due to bond stretching, bond angle bending,

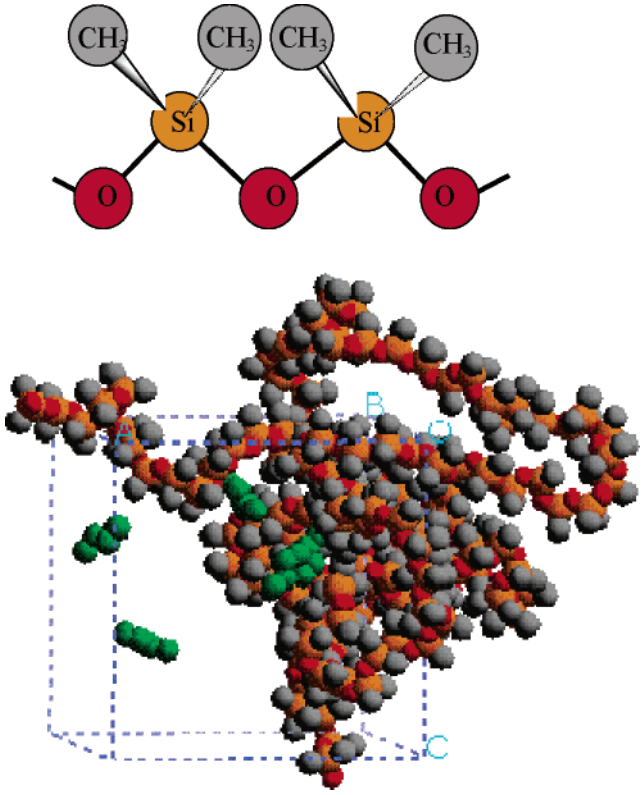

Figure 1. Schematic representation of PDMS examined in this work (top) and a representative configuration obtained from atomistic MD (bottom). The green molecules are *n*-butane molecules dissolved in the polymer.

dihedral angle torsion and nonbonded interactions between UAs in the same or different chains. In PDMS, nonbonded interactions consist of short range van der Waals repulsive and dispersive interactions and long range electrostatic (Coulombic) interactions. The functional form of the force field in terms of the potential energy is

$$V_{\text{total}}(\mathbf{r}_1,\ldots,\mathbf{r}_N) = V_{\text{stretching}} + V_{\text{bending}} + V_{\text{torsion}} + V_{\text{non-bonded}} = \sum_{\text{all bonds}} V(l_i) + \sum_{\text{all bond angles}} V(\theta_i) + \sum_{\text{all torsional angles}} V(\phi_i) + \sum_{\text{all pairs}} V(r_{ij}) = \sum_{\text{all bonds}} \frac{k_{l_i}}{2}(l_i - l_{i,o})^2 + \sum_{\text{all bond angles}} \frac{k_{\theta_i}}{2}(\theta_i - \theta_{i,o})^2 + \sum_{\text{all torsional angles}} \frac{1}{2}k_\phi(1 - \cos 3\phi) + \sum_{\text{all pairs}} \left(4\varepsilon_{ij}\left[\left(\frac{\sigma_{ij}}{r_{ij}}\right)^{12} - \left(\frac{\sigma_{ij}}{r_{ij}}\right)^{6}\right] + \frac{q_i q_j}{4\pi\varepsilon_o}\left(\frac{1}{r_{ij}} + \frac{(\varepsilon_s - 1)r_{ij}^2}{(2\varepsilon_s + 1)r_c^3}\right)\right) \quad (1)$$

where l_i, θ_i, and ϕ_i denote bond length, bond angle, and torsional angle respectively, r_{ij} is the distance between interaction sites i and j, and q_i is the partial charge on site i. Subscript o denotes parameter value at equilibrium. Flexible bonds are used and the potential energy of each bond is evaluated by using a simple harmonic potential (first term on the rhs of eq 1). Similarly, bond-angle fluctuations around the equilibrium angle are subject to harmonic fluctuations (second term on the rhs of eq 1). For all dihedral angles, a 3-fold symmetric torsional potential is used with $\phi = 0°$ denoting a *trans* state (third term on the rhs of eq 1). Finally, nonbonded interactions are described by a LJ potential for van der Waals interactions while the reaction field

Table 1. Atomistic UA Force Field for PDMS

Type of interaction	*Potential function and parameters*		
Bond stretching	$V_{\text{stretching}}(l) = \frac{1}{2}k_l(l-l_o)^2$		
	Bond	k_l (kcal/mol/Å^2)	l_o (Å)
	Si-O	700.2	1.64
	Si-CH_3	379.3	1.90
	O-CH_3 (terminal)	700.2	1.64
Bond bending	$V_{\text{bending}}(\theta) = \frac{1}{2}k_\theta(\theta-\theta_o)^2$		
	Bond angle	k_θ (kcal/mol deg^2)	θ_o (°)
	O-Si-O	0.0575	109.5
	O-Si-CH_3	0.0304	109.5
	CH_3-Si-CH_3	0.0304	109.5
	Si-O-Si	0.0153	144.0
	Si-O-CH_3 (terminal)	0.0153	144.0
Dihedral angles	$V_{\text{dihedral}} = \frac{1}{2}k_\phi(1-\cos 3\phi)$		
	Dihedral angle	k_ϕ (kcal/mol)	
	Si-O	1.8	
Non bonded Lennard-Jones	$V_{LJ}(r_{ij}) = 4\varepsilon_{ij}\left[\left(\frac{\sigma_{ij}}{r_{ij}}\right)^{12} - \left(\frac{\sigma_{ij}}{r_{ij}}\right)^{6}\right]$		
		σ (Å)	ε (kcal/mol)
	Si	3.385	0.585
	O	2.955	0.203
	CH_3	4.170	0.160
Non bonded electrostatic	$V_q(r_{ij}) = \left(\frac{q_i q_j}{4\pi\varepsilon_o}\right)\left(\frac{1}{r_{ij}} + \frac{(\varepsilon_s-1)r_{ij}^2}{(2\varepsilon_s+1)r_c^3}\right)$		
		Si	O	CH_3
	q (e)	0.3	-0.3	0.0

model[20] is used for the electrostatic interactions (last term on rhs of eq 1). Electrostatic are long range interactions that require special treatment in molecular simulation where the system examined is in the order of several hundred or, at the most, a few thousand interaction sites. The Ewald summation method and the reaction field model are the most widely used methods to account efficiently for electrostatic interactions.[20] In this work, the latter method was preferred because of its computational efficiency compared to the former. In eq 1, q_i and q_j are the partial charges of interaction sites i and j, ε_s is the dielectric constant of solvent, ε_o is the dielectric permittivity of vacuum (equal to 8.85419×10^{-12} C^2 J^{-1} m^{-1}), and r_c is the cutoff distance for the electrostatic interactions. LJ and electrostatic interactions are calculated for all UAs on different chains and between UAs on the same chain that are four or more bonds apart.

Standard Lorentz−Berthelot combining rules are used to describe nonbonded LJ interactions between sites of different type:

$$\varepsilon_{ij} = \sqrt{\varepsilon_{ii}\varepsilon_{jj}} \quad \text{and} \quad \sigma_{ij} = \frac{\sigma_{ii} + \sigma_{jj}}{2} \tag{2}$$

The starting point for the development of the new force-field for PDMS was the model proposed by Sok et al.[22] MD simulations at 300 K and 0.1 MPa resulted in a density value that was on the order of 10% higher than the experimental value. Consequently, the LJ parameters for the CH_3 UA were modified so that accurate density predictions are obtained from 300 up to 450 K and 0.1 MPa. This new parameter set was further used for MD simulations at higher pressures.

In terms of the bonded parameters of the model, it should be mentioned that, because the bond bending constant, k_{θ_i}, for angle Si−O−Si is relatively small (0.0087 kcal/mol deg^2) and the equilibrium bond angle is relatively large (144°) the probability that the bond angle goes over 180° cannot be neglected at high temperature.[25] Since the derivative of the potential functions with respect to the atom positions is not continuous at $\theta = 180°$, an energy jump occurs when the bond angle goes across 180°. To prohibit this jump, we increased the value of this constant by a factor of 2. This modification does not affect the thermodynamic and transport property values calculated through molecular simulation. To summarize, the parameters for the force field proposed for PDMS are listed in Table 1.

3. Simulation Details

All MD simulations were performed at the isobaric−isothermal (*NPT*) ensemble using the Nosé and Klein method.[32−34] In this case, the Lagrangian assumes the form

$$\mathcal{L} = \sum_i \frac{m_i}{2} s^2 \dot{r}_i^{\,2} - V_{\text{total}} + \frac{Q}{2}\dot{s}^2 - g k_B T \ln s + \frac{9}{2} W L^4 \dot{L}^2 - P_{\text{ext}} L^3 \tag{3}$$

where $g = 3nN_{\text{ch}} + 1$ is the number of degrees of freedom of the system, n is the number of atoms of each chain, N_{ch} is the number of chains, L is the box edge length, s is the "bath" degree of freedom used to control the temperature, W and Q are the inertia parameters associated with L and s, respectively, and P_{ext} is the externally set pressure. A fifth order Gear predictor−corrector scheme[35] is used to integrate the equations of motion in Cartesian coordinates. The values of the parameters W and Q are the same with those of previous work on poly(dimethylsilamethylene).[36,37]

All of the PDMS systems examined consisted of three chains of 80 monomer units. Thus, the molecular weight of the simulated polymer was equal to 5950. The end groups of the chains are methyl groups, so that the total charge of each chain is equal to zero. The initial configurations were obtained using the Cerius^2 software package of Accelrys Inc. Polymer chains were built in an amorphous cell using periodic boundary conditions. These initial configurations were subjected to molecular mechanics.[38] Energy minimization took place in two stages. First, the steepest descent method was used with maximum number of iterations equal to 100 followed by the conjugate gradient method with maximum number of iterations up to 10 000. MD simulations were performed with an integration time step of 0.5 fs to ensure system stability over time. The "equilibration" MD stage was 1 ns long, while the production run was 5 ns. The major criteria used to ensure equilibration are related to conformational characteristics of the chains (i.e., smooth dihedral angle distribution) and to stability of running averages for the total energy and its constituents and the density of the system. In order to improve statistics in the calculated physical properties, for each state point several (four to six, depending on the conditions) runs were performed starting from different initial configurations. In each run, 5000 configurations were recorded at equal time intervals and they were used for the calculation of the thermodynamic and of the structural properties of polymer melt. Furthermore, they were used for the evaluation of the chemical potential of *n*-alkanes, *n*-perfluoroalkanes, and noble and light gases in PDMS. Periodic

Table 2. Atomistic UA Force Field for *n*-Alkanes and *n*-Perfluoroalkanes

Type of interaction	*Potential function and parameters*	
	n-Alkanes[42]	
Bond bending	$V_{\text{bending}}(\theta) = \frac{1}{2}k_\theta(\theta - \theta_o)^2$	$k_\theta = 0.038$ kcal/mol deg^2 $\theta_o = 114$ °
Dihedral angles	$V_{dihedral} = \sum_{i=1}^{3}\alpha_i\left[1 + (-1)^{i+1}\cos(i\phi)\right]$	$\alpha_1/k_B = 355.03$ K $\alpha_2/k_B = -68.19$ K $\alpha_3/k_B = 791.32$ K
Lennard - Jones	$V_{LJ}(r_{ij}) = 4\varepsilon_{ij}\left[\left(\frac{\sigma_{ij}}{r_{ij}}\right)^{12} - \left(\frac{\sigma_{ij}}{r_{ij}}\right)^{6}\right]$	$\sigma_{CH_4} = 3.73$ Å $\varepsilon_{CH_4} = 148$ K $\sigma_{CH_3} = 3.75$ Å $\varepsilon_{CH_3} = 98$ K $\sigma_{CH_2} = 3.95$ Å $\varepsilon_{CH_2} = 46$ K
	n-Perfluoroalkanes[43,46]	
Bond bending	$V_{\text{bending}}(\theta) = \frac{1}{2}k_\theta(\theta - \theta_o)^2$	$k_\theta = 0.038$ kcal/mol deg^2 $\theta_o = 114.6$ °
Dihedral angles	$V_{dihedral} = \sum_{i=0}^{7}\alpha_i\cos^i\phi$	$\alpha_0/k_B = 595.4$ K, $\alpha_4/k_B = -7875.3$ K $\alpha_1/k_B = -282.7$ K, $\alpha_5/k_B = -14168$ K $\alpha_2/k_B = 1355.2$ K, $\alpha_6/k_B = 9213.7$ K $\alpha_3/k_B = 6800$ K, $\alpha_7/k_B = 4123.7$ K
Lennard - Jones	$V_{LJ}(r_{ij}) = 4\varepsilon_{ij}\left[\left(\frac{\sigma_{ij}}{r_{ij}}\right)^{12} - \left(\frac{\sigma_{ij}}{r_{ij}}\right)^{6}\right]$	$\sigma_{CF_4} = 4.66$ Å $\varepsilon_{CF_4} = 134$ K $\sigma_{CF_3} = 4.60$ Å $\varepsilon_{CF_3} = 60$ K $\sigma_{CF_2} = 4.60$ Å $\varepsilon_{CF_2} = 30$ K

boundary conditions were applied to the simulation box. A Verlet neighbor list[20] and a truncated LJ and electrostatic potential were used to speed up calculations of interactions between molecules. In this work, the LJ potential tail beyond $r = 1.45\sigma$ was substituted by a fifth order polynomial, whose value beyond $r = 2.33\sigma$ is equal to zero. For electrostatic interactions, the cutoff distance, r_c, was equal to 13.5 Å, a value which is smaller than half the box edge length. The dielectric constant of solvent, ε_s, was equal to infinity, assuming conducting boundary conditions. The instantaneous pressure of the system P_{int} was calculated during the simulation according to the molecular virial expression proposed by Theodorou et al.[39] The "tail" contributions to the internal energy and to the pressure were taken into account.[20]

The chemical potential was calculated using the Widom's test particle insertion method.[40] According to Widom's method, one inserts a "ghost" molecule at a random position into the simulated system and calculates its interaction energy with the other molecules. This interaction energy is directly related to the excess chemical potential, μ^{ex}, of the "ghost" molecule. In the *NPT* ensemble, μ^{ex} is calculated by the expression[41]

$$\mu_{ex} = \mu - \mu^{ig} = -\frac{1}{\beta}\ln\left[\frac{1}{\langle V\rangle_{NPT}}\langle V\langle\exp(-\beta V_{\text{ghost}}^{\text{intra}} - \beta V_{\text{ghost}}^{\text{inter}})\rangle_{\text{Widom}}\rangle_{NPT}\right] + \frac{1}{\beta}\ln\langle\exp(-\beta V_{\text{ghost}}^{\text{intra}})\rangle_{\text{ideal gas}} \quad (4)$$

where $\beta = 1/k$T, $V_{\text{ghost}}^{\text{inter}}$ is the intermolecular energy and $V_{\text{ghost}}^{\text{intra}}$ is the intramolecular energy of the "ghost" molecule. The latter is calculated independently in a single chain simulation. V is the instantaneous volume of the system and the brackets denote ensemble averaging over all configurations and spatial averaging over all "ghost" molecule positions.

Table 3. Force Field Parameters for Noble and Light Gases

gas	σ (Å)	ε (kcal/mol)	l (Å)
He[a]	2.57	0.020	
Ne[a]	2.76	0.067	
Ar[a]	3.41	0.236	
Kr[a]	3.59	0.344	
Xe[a]	4.07	0.448	
N_2[b]	3.31	0.074	1.09
O_2[c,d]	3.09	0.089	1.21

[a] Taken from ref 47. [b] Taken from ref 48. [c] Taken from ref 49. [d] Taken from ref 50.

In the present work, Widom's method was used for the calculation of μ_{ex} of *n*-alkanes (CH_4 to *n*-C_6H_{14}), *n*-perfluoroalkanes (CF_4 to *n*-C_4F_{10}), noble gases (He, Ne, Ar, Kr, Xe) and light gases (N_2, O_2) in PDMS. *n*-alkanes were modeled using the TraPPE force field, a very accurate UA model developed by Siepmann and co-workers[42] for linear and branched hydrocarbons, alcohols, and many other organic compounds. In the TraPPE model, bond lengths are kept constant and equal to 1.54 Å. In Figure 1, a typical equilibrated configuration of the polymer matrix with *n*-butane molecules inserted is shown.

In the case of *n*-perfluoroalkanes, CF_2 and CF_3 groups were treated as UA with effective LJ well depth and size parameters.

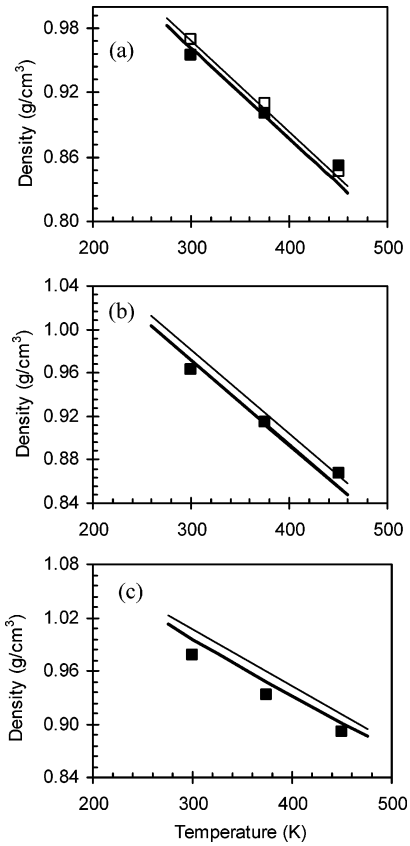

Figure 2. Melt density of PDMS at (a) 0.1, (b) 10, and (c) 40 MPa at different temperatures: Experimental data (open squares from ref 6; thick line, from ref 3; thin line from ref 4) and MD simulations (solid squares).

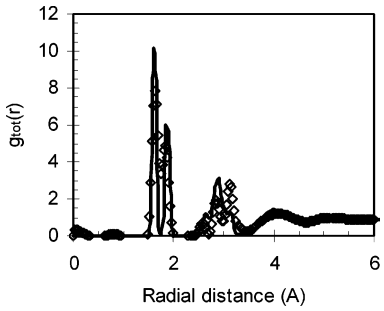

Figure 3. Total pair distribution function at 300 K and 0.1 MPa for PDMS. Experimental data (points)[28] and MD simulations (line).

The T-model proposed by Cui et al.[43] optimized for vapor−liquid equilibrium calculations of pure perfluoroalkanes and applied[44] to high-pressure vapor−liquid equilibrium calculations of perfluoroalkanes with carbon dioxide was adopted. In this work, the CF_3 LJ energy parameter was set equal to 60 K so that a good prediction of the infinite dilution solubility coefficient of C_2F_6 in PDMS at 300 K was obtained, and used subsequently for all perfluoroalkanes. According to this model, the C−C bond lengths are fixed at 1.54 Å, corresponding to the experimental bond length for the crystalline polytetrafluoroethylene.[45] For the spherical CF_4, LJ parameters proposed by Reid et al.[46] determined from viscosity data were adopted. In Table 2, the force-field parameters for *n*-akanes and *n*-perfluoroalkanes used in this work are reported.

All of the noble gases were treated as spherical molecules and the force field parameters proposed by Hirschfelder et al.[47] based on second virial coefficient data were used. Nitrogen and oxygen were modeled as diatomic molecules with constant bond

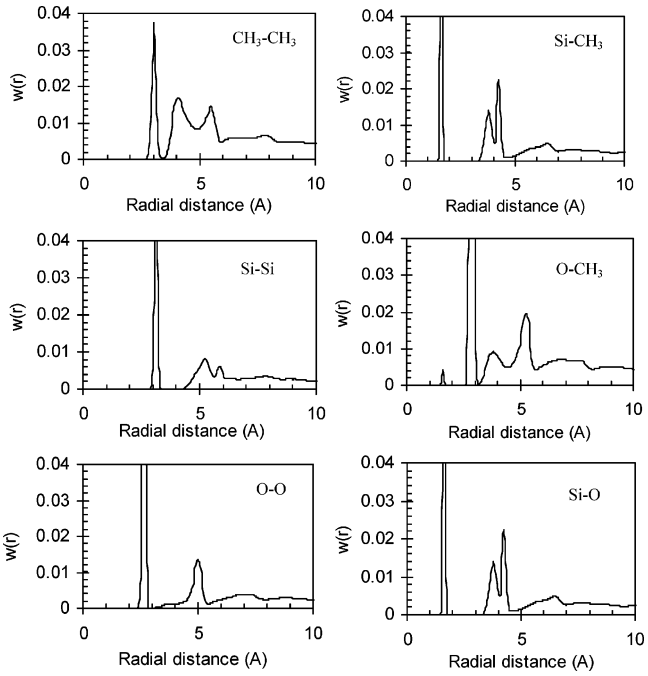

Figure 4. Intramolecular pair density function at 300 K and 0.1 MPa for PDMS obtained from MD simulation.

length. For nitrogen, the potential model proposed by Cheung et al.[48] obtained by fitting liquid experimental thermodynamic data at various temperatures and pressures was adopted. Finally for oxygen, equilibrium bond length value l_o and LJ parameters proposed by Huber et al.[49] and Powles et al.,[50] respectively, were used. Overall, the force field parameters for noble and light gases are reported in Table 3.

From the excess chemical potential, one may calculate the Henry's law constant of the solute in polymer, according to the expression

$$H_{solute\to pol} = \lim_{x_{solute}\to 0}\left(\frac{\rho_{pol}}{\beta}\exp(\beta\mu^{ex}_{solute})\right) \qquad (5)$$

where ρ_{pol} is the density of the polymer. Alternatively, the solubility coefficient, S_o at infinite dilution can be calculated from the expression:

$$S_o = \frac{22400\ \text{cm}^3\text{(STP)/mol}}{RT}\lim_{x_{solute}\to 0}\exp(-\beta\mu^{ex}_{solute}) \qquad (6)$$

In this work, calculations are reported in terms of S_o in units of cm^3(STP)/(cm^3 pol atm) that are used widely in membrane science and technology. STP corresponds to an absolute pressure of 101.325 kPa and a temperature of 273.15 K.

4. Results and Discussion

A. Thermodynamic Properties. Initially, the new force field is tested for the prediction of PDMS melt density at various temperatures and pressures. MD simulations were performed at 300, 375, and 450 K and for each temperature at 0.1, 10, and 40 MPa. Experimental data from different sources are reported in the literature.[3,4,6] Data from refs 3 and 4 cover an extended temperature and pressure range. In all cases, a systematic difference in the density on the order of 0.5−0.6% is observed between the two sources. The deviation increases at higher pressures. In Figure 2, experimental and simulated melt density of PDMS is shown as a function of temperature

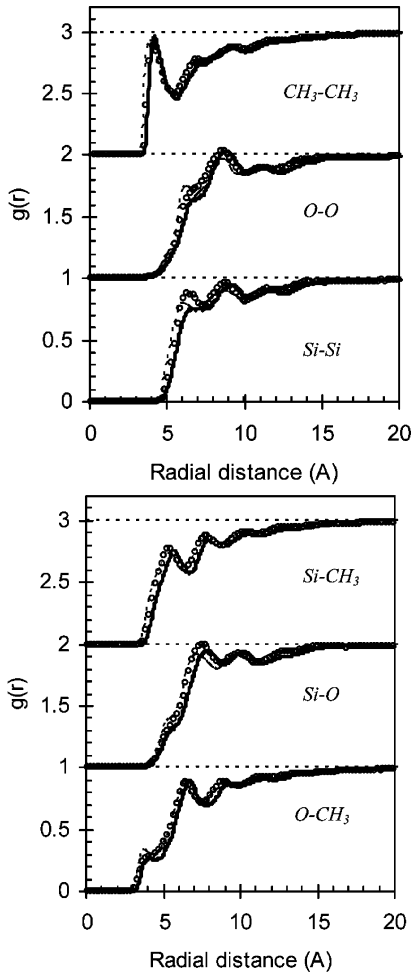

Figure 5. Intermolecular pair distribution function at 300 K and 0.1 MPa for PDMS for like (top) and unlike (bottom) pairs obtained from MD using the new model (solid lines). Open circles are calculations using the hybrid/UA model of Frischknecht and Curro[27] and dotted lines are calculations from Frischknecht and Curro[27] using the UA/CI model of Sok et al.[22]

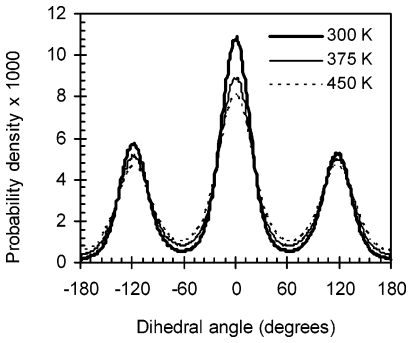

Figure 6. Distribution of Si−O−Si−O dihedral angle as a function of temperature from MD simulation.

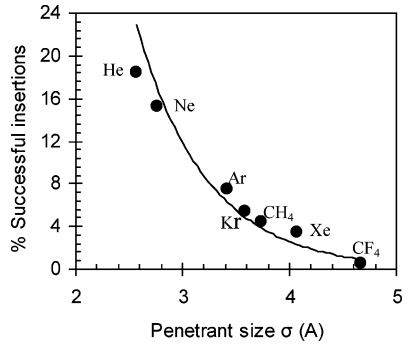

Figure 7. Percentage of successful insertions as a function of penetrant size at 300 K. The curve is an exponential fit to the simulation data.

Table 4. Percentage of Successful Insertions of Solutes in PDMS at 300 and 450 K, and 0.1 MPa

gas	300 K	450 K	gas	300 K	450 K	gas	300 K	450 K
CH_4	4.5	10.4	CF_4	0.6	3.9	He	18.4	26.5
C_2H_6	2.4	7.5	C_2F_6	0.4	2.7	Ne	15.2	23.3
C_3H_8	1.2	5.1	C_3F_8	0.2	1.6	Ar	7.5	13.9
n-C_4H_{10}	0.6	3.9	n-C_4F_{10}	0.08	1.2	Kr	5.4	11.8
n-C_5H_{12}	0.3	3.1				Xe	3.4	7.4
n-C_6H_{14}	0.2	2.4				N_2	6.0	12.9
						O_2	8.2	15.5

and pressure. MD predictions are in excellent agreement with either of the experimental data sets at 0.1 MPa while some deviations are observed at higher pressures.

An additional thermodynamic property examined is the solubility parameter of the polymer melt calculated from the following expression:

$$\delta = \sqrt{\frac{E_{coh}}{V}} \tag{7}$$

E_{coh} is the cohesive energy of the system and is estimated as the difference between the intramolecular energy of all "parent" chains and the total potential energy of the simulation box, by taking potential "tail" contributions into account.[51] The solubility parameter, δ, from MD at 300 K and 0.1 MPa is equal to 6.63 $\pm$ 0.01 $(cal/cm^3)^{1/2}$ while the experimental value[52] is equal to 7.3 $(cal/cm^3)^{1/2}$. Obviously, the new force field is not able to predict δ of PDMS very accurately.

B. Structural Properties. Fluid structure at the microscopic level is typically characterized by the radial distribution function $g(r)$, which is the probability of finding an atom at distance r from the reference atom with reference to the bulk of the fluid. In other words: $g(r) = \rho(r)/\rho_o$ where $\rho(r)$ is the local density and ρ_o is the bulk density.

For the case of polymers, the total radial distribution function $g_{tot}(r)$ is a sum of contributions due to atoms (in the representation used here, an atom is equivalent to united atom) in the same chain with the reference atom or in different chains. In the first case, we refer to intramolecular pair density function, $w(r)$, while in the second case we refer to intermolecular pair distribution function, $g(r)$. In Figure 3, the total pair distribution function, $g_{tot}(r)$, at 300 K and 0.1 MPa is presented. Experimental X-ray scattering data from Sides et al.[28] are shown for comparison. Good agreement between experiment and simulation is observed, both in terms of peak position as well as peak intensity. A small difference on the peak position by about 0.2 Å is observed for the third peak.

The intramolecular pair density function and the intermolecular distribution function can be calculated for individual pairs of UAs. For PDMS, no experimental data were found in the literature for comparison. Instead, comparisons are made with previous molecular simulation work by other researchers.

In Figures 4 and 5, $w(r)$ and $g(r)$ are shown for all the individual pairs of the same (Si−Si, O−O, and CH_3−CH_3) or different (Si−O, Si−CH_3, and O−CH_3) types of UAs. The $w(r)$ and $g(r)$ functions presented here agree well with previous molecular simulations studies of Sok[53] and Frischknecht and Curro,[27] respectively, concerning the individual peak positions and intensities. It should be pointed out that the differences in absolute values of $w(r)$ between this work and the work of Sok[53] should be attributed to different normalization of the raw data used in each case. For the $g(r)$ distribution (Figure 5), small

Table 5. Experimental Data and Molecular Simulation Results at 300 and 450 K and 0.1 MPa for the Infinite Dilution Solubility Coefficients S_o (cm^3 (STP)/cm^3 pol atm) of *n*-Alkanes in PDMS

	n-alkanes					
	CH_4	C_2H_6	C_3H_8	*n*- C_4H_{10}	*n*-C_5H_{12}	*n*-C_6H_{14}
			MD Simulation			
300 K	0.47 ± 0.01	2.6 ± 0.1	7.1 ± 0.4	21 ± 2	62 ± 14	191 ± 86
450 K	0.33 ± 0.01	0.75 ± 0.01	1.22 ± 0.01	1.98 ± 0.01	3.1 ± 0.1	4.8 ± 0.1
			Experiment			
283 K[7]	0.61		13.51			
295 K[8]	0.6	3.2	7.7	14		
298 K[9]	0.525	3.01				
298 K[10]	0.436	2.34	7.52	21.9	64.4	
300 K[11]	0.56					
301 K[15]	0.38					
303 K[16]					63.5	
303 K[12]				21.4	62.2	
308 K[13]	0.42	2.2	5.0			
308 K[7]	0.45		6.45			
308 K[14]	0.43					
423 K[6]					3.4	

differences in relative intensities of peaks are due to different LJ parameters used in each case. Furthermore, Frischknecht et al.[27] used a LJ 9−6 potential instead of the 12−6 potential used here. Frischknecht et al.[27] also proposed an explicit-atom force field for PDMS that was in good agreement with these other force fields concerning the $g(r)$ calculations.

A standard approach to characterize the conformation of flexible macromolecules is based on the backbone dihedral angle distribution.[31,54] Simulation results for the Si−O−Si−O dihedral angle distribution of PDMS are shown in Figure 6. The distribution shows a clear preference for the trans state (at 0°) with local maxima in gauche$^+$ (at 120°) and gauche$^-$ (at −120°) conformations, very similar to polyethylene.[54] As the temperature increases, peak heights decrease and the distribution broadens which is a typical behavior for all chain fluids. Calculations presented here agree very well with MD calculations for a dimethylsiloxane oligomer composed of eight monomer units reported by Bahar et al.[55]

C. Solubility in PDMS. PDMS melt configurations generated by MD were used for the calculation of solubility of various components in the polymer. The Widom test particle insertion method[40] was used to calculate the excess chemical potential of *n*-alkanes, *n*-perfluoroalkanes, and noble and light gases in PDMS at various temperature and pressure values. To overcome problems associated with the slow relaxation of long chain polymer molecules that is not captured effectively by MD techniques and may affect the μ^{ex} calculations, six, two, and four initially different structures at 300, 375, and 450 K, respectively, were examined. At higher pressures (10 and 40 MPa) and 300 K four initially different structures were examined. In each of the 5000 PDMS configurations stored during the MD simulation of the polymer melt, a large number of molecule insertions were attempted. For the case of penetrant molecules with more than three UAs, that is *n*-butane, *n*-pentane, *n*-hexane, and *n*-perfluorobutane, molecule insertions were performed using configuration bias techniques.[41] An insertion is defined as "successful" in the case where $r_{solute-pol} > 0.7\ \sigma_{solute-pol}$ for all solute − polymer segment pairs, where $r_{solute-pol}$ is the distance between a segment of the inserted solute molecule and a polymer segment and $\sigma_{solute-pol}$ is the LJ parameter for this pair of segments.[36] The number of attempted insertions used per polymer configuration was as follows: 10 000 for monatomic species (CH_4, CF_4, He, Ne, Ar, Kr, Xe), 20 000 for diatomic species (C_2H_6, C_2F_6, N_2, O_2), 50 000 for propane and perfluoropropane, 100 000 for *n*-butane and *n*-perfluorobutane, 200 000 for *n*-pentane, and 400 000 for *n*-hexane.

In Table 4, the rate of successful insertions for different solutes at 300 and 450 K is shown. As expected, for small or light solute molecules the rate of successful insertions is higher than for the large or heavy solute molecules. *n*-Perfluoroalkane successful insertions are lower than those of their hydrocarbon analogs, consistent with the larger size of the fluorocarbons. In addition, at 450 K the successful insertion rate is higher, mainly due to lower polymer density and thus to higher free volume. The increase is more pronounced for the heavier solutes. More specifically, for the smaller alkanes (methane to *n*-butane) and for the noble and light gases an increase by a factor of 2−6 is observed, while for the larger alkanes (*n*-pentane and *n*-hexane) the rate of successful insertions is an order of magnitude higher. In the case of *n*-perfluoroalkanes, the ratio of the successful insertions at the two temperatures is even higher (about 7 times for perfluoromethane to perfluoropropane and more than an order of magnitude for *n*-perfluorobutane). In Figure 7, the percentage of successful insertions as a function of penetrant size is shown for monatomic penetrants. At high enough penetrant size, the number of successful insertions approaches zero.

In Table 5, experimental data in the temperature range 283−308 K (and 423 K for *n*-pentane)[6−16] and MD simulation results at 300 and 450 K and 0.1 MPa for the solubility coefficient at infinite dilution, S_o, of *n*-alkanes in PDMS are shown. The agreement between experiment and simulation is very good in all cases. The solubility coefficient S_o decreases at higher temperatures which is more pronounced for the case of heavier *n*-alkanes, indicating that the sorption process is exothermic. Similar behavior has been observed experimentally for the case of various *n*-alkanes in poly(dimethylsilamethylene)[36] and α-olefins in low-density polyethylene.[56] The statistical uncertainty reported in the simulations is the standard deviation in the calculated values for the different structures. For the larger of the *n*-alkanes at 300 K, the statistical uncertainty remains high despite the many different structures examined and the large number of molecule insertions. This should be attributed to the very low successful insertion rate. In Figure 8, experimental data and MD predictions for S_o are shown. For clarity, at 300 K only the experimental data reported by Kamiya et al.[10] are presented, since these authors performed a very thorough experimental investigation for very many (34 in total) different penetrants at conditions close to the one examined here.

For the case of *n*-pentane solubility in PDMS, experimental data using different techniques (pressure decay[6] and inverse gas chromatography[16]) over a wide temperature range are reported

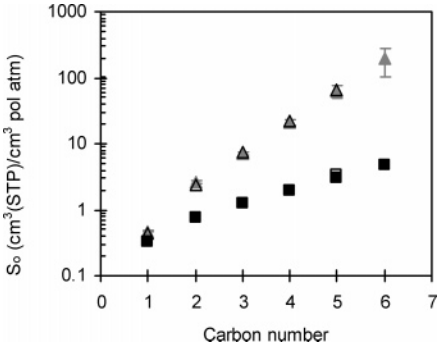

Figure 8. Infinite dilution solubility coefficient S_o (cm^3(STP)/cm^3 pol atm) of *n*-alkanes in PDMS at 300 K (gray triangles) and 450 K (solid squares) and 0.1 MPa from MD simulation. Open symbols are experimental data from ref 10 (298 K) and from ref 6 (423 K).

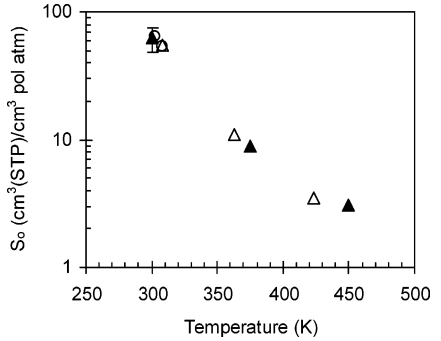

Figure 9. Temperature dependence of the solubility coefficient S_o of n-pentane in PDMS. Closed symbols are MD results. Statistical uncertainty in MD values at 375 and 450 K is much less than the size of the symbols. Experimental data: open triangles are from pressure decay measurements,[6] and open circles are from inverse gas chromatography.[16]

Table 6. Pressure Effect of the Solubility Coefficient of *n*-alkanes in PDMS at 300 K

	S_o (cm^3 (STP)/cm^3 pol atm)				
P (MPa)	CH_4	C_2H_6	C_3H_8	*n*-C_4H_{10}	*n*-C_5H_{12}
10	0.44 ± 0.05	2.5 ± 0.5	7 ± 2	20 ± 6	42 ± 5
40	0.301 ± 0.005	1.4 ± 0.1	4.0 ± 0.4	11 ± 4	25 ± 5

Table 7. Experimental Data and Molecular Simulation Results at 300 and 450 K and 0.1 MPa for the Infinite Dilution Solubility Coefficients S_o (cm^3 (STP)/cm^3 pol atm) of *n*-perfluoroalkanes in PDMS

	n-perfluoroalkane			
	CF_4	C_2F_6	C_3F_8	*n*- C_4F_{10}
	MD Simulation			
300 K	0.28 ± 0.06	0.35 ± 0.01	0.97 ± 0.01	2.6 ± 0.4
450 K	0.21 ± 0.01	0.21 ± 0.01	0.34 ± 0.01	0.58 ± 0.02
	Experiment			
298 K[10]	0.166	0.382	0.803	
308 K[13]	0.19	0.33	0.85	

in the literature. MD simulations at 375 K were performed in addition to 300 and 450 K and are compared to experimental data in Figure 9. The temperature dependence of S_o is quite strong; a decrease in S_o by approximately 20 times is observed over 150 K. The agreement between experimental data using different techniques and MD simulation is excellent.

The effect of pressure on the infinite dilution solubility coefficient S_o of *n*-alkanes in PDMS was also examined. In Table 6, simulation results are reported. No experimental data are available at these conditions. It is obvious that as the pressure increases the solubility coefficient decreases. This behavior is due to the higher density of the polymer melt at elevated pressures.

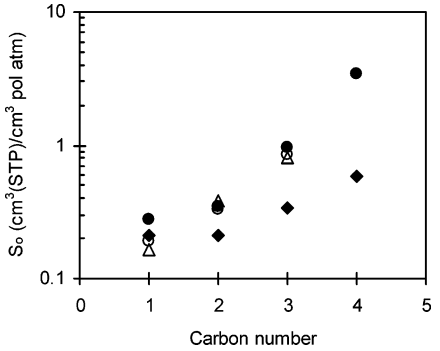

Figure 10. Solubility coefficients S_o of *n*-perfluoroalkanes in PDMS at 300 K (solid circles) and 450 K (solid diamonds) and 0.1 MPa. Experimental data are from Kamiya et al.[10] (open circles at 298 K) and from Merkel et al.[13] (open triangles at 308 K).

In Table 7, the infinite dilution solubility coefficients of *n*-perfluoroalkanes in PDMS at 300 and 450 K and 0.1 MPa together with literature experimental values at 298 and 308 K are shown.[10,13] The agreement between simulation and experiment is good, with the exception of CF_4, where simulation overestimates the experimental value by approximately 50%. This failure should be attributed to the force field parameters for CF_4 that were obtained from fitting viscosity data.[46] Comparison between experiment and simulation for S_o of *n*-perfluoroalkanes is shown in Figure 10. It should be mentioned that *n*-perfluoroalkanes are less soluble than the analogous hydrocarbon molecules in PDMS. Similar experimental results have been reported for a few fluorinated gases in PDMS by several researchers.[10,13,17]

Finally, the infinite dilution solubility coefficients of five noble and two light gases in PDMS at 300, 375, and 450 K and 0.1 MPa were calculated. In Table 8, MD simulation results and experimental data from different sources[9,10,13−15,18,19] are presented. Despite the scattering in experimental data, the agreement between experiment and simulation is remarkably well in most cases. The solubility coefficients S_o of these gases as a function of the experimental gas critical temperature are plotted in Figure 11. For clarity again, only the experimental data of Kamiya et al.[10] are presented. Experimental data indicate that, in general, gas solubility in polymers is correlated very accurately with the gas critical temperature. This empirical correlation is verified by the MD calculations presented here (solid line in Figure 11).

Furthermore, if one plots S_o vs the critical temperature for all the solutes examined here, then data can be grouped in two sets, as shown in Figure 12. The first set of data refers to *n*-perfluoroalkanes while the second set contains the remaining of the solutes. A linear fit to the second set of data results in a slope for $d(\log S_o)/dT_c$ equal to 0.007, in very good agreement with a slope of 0.0076 reported by Kamiya et al.[10] for 33 gases in PDMS, of 0.0062 reported by Merkel et al.[13] for 7 gases (H_2, O_2, N_2, CO_2, CH_4, C_2H_6, C_3H_8) in PDMS, and of 0.0071 reported by van Amerongen[57] for 7 gases (H_2, O_2, N_2, CO_2, CH_4, NH_3, SO_2) in natural rubber.

Finally, the temperature dependence of S_o shows a systematic variation from positive to negative as the size of the gas molecule increases, as shown in Figure 13. MD calculations indicate that the temperature coefficient of S_o is positive for He and Ne, close to zero for Ar, N_2 and O_2 and negative for CH_4, Kr and Xe. A qualitatively similar behavior has been observed experimentally by van Amerongen[58] for various gases

Table 8. Solubility Coefficients S_o (cm³ (STP)/cm³ pol atm) of Noble and Light Gases in PDMS at 0.1 MPa Obtained from MD Simulation and Experiment[a]

	S_o (cm³ (STP)/cm³ pol atm)			
gas	300 K	375 K	450 K	experiment
He	0.058 ± 0.001	0.091 ± 0.001	0.125 ± 0.001	0.028 (ref 10), 0.046 (ref 18), 0.043 (ref 19)
Ne	0.078 ± 0.001	0.109 ± 0.001	0.139 ± 0.001	0.042 (ref 10)
Ar	0.31 ± 0.02	0.27 ± 0.01	0.26 ± 0.01	0.256 (ref 9), 0.225 (ref 10), 0.34 (ref 19)
Kr	0.76 ± 0.04	0.58 ± 0.02	0.47 ± 0.02	0.586 (ref 10)
Xe	2.8 ± 0.2	1.4 ± 0.1	0.9 ± 0.1	1.92 (ref 10)
N_2	0.15 ± 0.01	0.15 ± 0.01	0.16 ± 0.01	0.127 (ref 9), 0.09 (ref 13), 0.111 (ref 10), 0.12 (ref 14), 1.1 (ref 15)
O_2	0.22 ± 0.01	0.21 ± 0.01	0.19 ± 0.01	0.224 (ref 9), 0.18 (ref 13), 0.205 (ref 10)

[a] Temperatures are as follows: ref 10, 298 K; ref 18, 300 K; ref 19, 273 K; ref 9, 298 K; ref 13, 308 K; ref 14, 308 K; ref 15, 301 K.

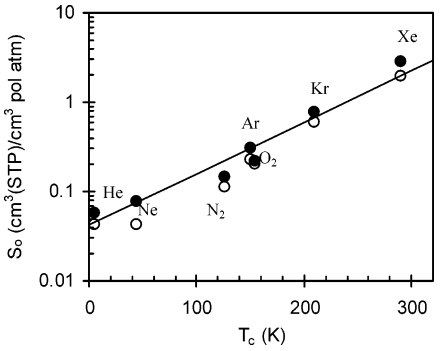

Figure 11. Infinite dilution solubility coefficient of light gases in PDMS at 300 K and 0.1 MPa obtained from MD simulation (solid circles). Open symbols are experimental data.[10] The solid line is a fit to simulation data.

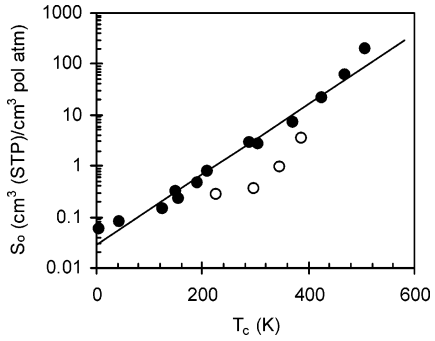

Figure 12. Correlation of infinite dilution solubility coefficient, S_o, in PDMS with penetrant critical temperature: Solid circles correspond to hydrocarbons and noble and light gases results from this work; open circles correspond to *n*-perfluoroalkanes results from this work.

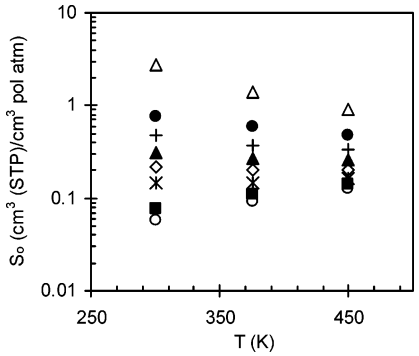

Figure 13. Infinite dilution solubility coefficient S_o of noble and light gases in PDMS as a function of temperature obtained from MD simulation (He, open circles; Ne, solid squares; N_2, stars; O_2, open diamonds; Ar, solid triangles; CH_4, crosses; Kr, solid circles; Xe, open triangles).

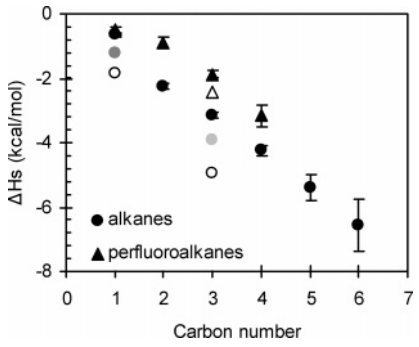

Figure 14. Enthalpy of sorption of *n*-alkanes and *n*-perfluoroalkanes in PDMS. Solid symbols: MD simulations. Experimental data: open circles from Shah et al.[7] gray circles from Kamiya et al.,[10] and open triangles and light gray circles from Prabhakar et al.[17]

in natural rubber and by Curro et al.[59] for noble gases in polyethylene using the polymer reference interaction site (PRISM) model.

Simulation results for S_o at different temperatures can be used for the calculation of the enthalpy of sorption (ΔH_s) of solutes in PDMS, according to the expression:

$$\frac{\partial(\ln S_o)}{\partial\left(\frac{1}{T}\right)} = -\frac{\Delta H_s}{R} \tag{8}$$

Results are shown in Figure 14 for *n*-alkanes and *n*-perfluoroalkanes together with experimental values proposed by Shah et al.[7] for methane and propane, by Kamiya et al.[10] for methane and experimental values for the isosteric enthalpy of sorption of propane and of perfluoropropane reported by Freeman and co-workers.[17] An almost linear increase, in absolute terms, with carbon number is observed for ΔH_s, that has been reported also for other silicon-containing polymers.[36] *n*-Alkanes exhibit a higher $-\Delta H_s$ value than their corresponding perfluoroalkanes and this is confirmed both experimentally and computationally. In all cases, MD results are lower, in absolute terms, than the few experimental values which, in turn, deviate from each other.

5. Conclusions

In this work, the thermodynamic properties and microscopic structure of PDMS melt were examined using molecular dynamics. For this purpose, an accurate force field was used that was developed based on Sok et al.[22] model. Force field development aimed toward the accurate representation of polymer melt density over a wide temperature range at ambient pressure. The force field was also used for melt density prediction at high pressures (10 and 40 MPa). Model predictions and experimental data were in good agreement in all cases. The microscopic structure of polymer melt was also studied in detail.

Subsequently, the solubility of *n*-alkanes, *n*-perfluoroalkanes, and noble and light gases in PDMS at 300, 375, and 450 K was calculated using the Widom test particle insertion technique.

Accurate force fields were used for the solute molecules. Results agreed very well with available experimental data, mostly around 300 K with few scatter data at higher temperatures, with the exception of CF_4. A systematic variation of temperature effect on gas solubility from positive, for the case of relatively lighter gases, to negative, for the case of relatively heavier gases, was observed. Work in this topic is underway for the case of other silicon-containing polymers. MD results for the solubility coefficient at various temperatures were used for the calculation of enthalpy of sorption of *n*-alkanes and *n*-perfluoroalkanes in PDMS. Calculations were in good agreement with limited experimental data available from the literature.

Acknowledgment. Financial support of this project through the European Union−European Social Fund, the Greek Secretariat of Research and Technology and Bayer Technology Services GmbH is gratefully acknowledged. We are thankful to Dr. John Curro of Sandia National Laboratories for many helpful suggestions and criticism regarding this work and for providing the $g(r)$ calculations for PDMS shown in Figure 5, Dr. Antony Habenschuss of Oak Ridge National Laboratory for providing the experimental X-ray scattering data for PDMS shown in Figure 3, and Dr. Oliver Pfohl of Bayer Technology Services GmbH, Germany, for helpful comments regarding this work. I.G.E. is thankful to the Technical University of Denmark, Department of Chemical Engineering, IVC−SEP, for a visiting professorship funded by The Danish Research Council for Technology and Production Sciences during the last part of this work.

Note Added after ASAP Publication. This article was released ASAP on February 9, 2007. In the last section of Table 1, an equation has been added. The corrected version was posted on February 15, 2007.

References and Notes

(1) Paul, D. R., Yampolskii, Yu. P., Eds. *Polymeric Gas Separation Membranes*; CRC Press: Boca Raton, FL, 1994.
(2) Dohrn, R.; Pfohl, O. Entfernen von Flüchtigen aus Polymeren: Physikalische Grenzen. in *Aufbereitungstechnik 2006*, VDI Verlag: Düsseldorf, Germany, 2006.
(3) Fakhreddine, Y. A.; Zoller, P. *J. Appl. Polym. Sci.* **1990**, *41*, 1087.
(4) Shih, H.; Flory, P. J. *Macromolecules* **1972**, *5*, 758.
(5) Dee, G. T.; Ougizawa, T.; Walsh, D. J. *Polymer* **1992**, *33*, 3462.
(6) Pfohl, O.; Riebesell, C.; Dohrn, R. *Fluid Phase Equilib.* **2002**, *202*, 289.
(7) Shah, V. M.; Hardy, B. J.; Stern, S. A. *J. Polym. Sci., B: Polym. Phys.* **1986**, *24*, 2033.
(8) Yampolskii, Y.; Durgaryan, S. G.; Nametkin, N. S. *Vysokomol Soed, B* **1979**, *21*, 616.
(9) Kamiya, Y.; Naito, Y.; Hirose, T.; Mizoguchi, K. *J. Polym. Sci., B: Polym. Phys.* **1990**, *28*, 1297.
(10) Kamiya, Y.; Naito, Y.; Terada, K.; Mizoguchi, K.; Tsuboi, A. *Macromolecules* **2000**, *33*, 3111.
(11) Ichiraku, Y.; Stern, S. A.; Nakagawa, T. *J. Membr. Sci.* **1987**, *34*, 5.
(12) Robb, W. L. *Ann. N.Y. Acad. Sci.* **1968**, *146*, 119.
(13) Merkel, T. C.; Bondar, V. I.; Nagai, K.; Freeman, B. D.; Pinnau, I. *J. Polym. Sci., B: Polym. Phys.* **2000**, *38*, 415.
(14) Pope, D. S.; Sanchez, I. C.; Koros, W. J.; Fleming, G. K. *Macromolecules* **1991**, *24*, 1779.
(15) Tremblay, P.; Savard, M. M.; Vermette, J.; Paquin, R. *J. Membr. Sci.* **2006**, *282*, 245.
(16) Krüger, K.-M.; Pfohl, O.; Dohrn, R.; Sadowski, G. *Fluid Phase Equilib.* **2006**, *241*, 138.
(17) Prabhakar, R. S.; Merkel, T. C.; Freeman, B. D.; Imizu, T.; Higuchi, A. *Macromolecules* **2005**, *38*, 1899.
(18) Pauly, S. In *Polymer Handbook*, 3rd ed.; Brandrup, J., Immergut, E. H., Eds.; Wiley: New York, 1989.
(19) Barrer, R. M.; Chio, H. T. *J. Polym. Sci., C* **1965**, *10*, 111.
(20) Allen, M. P.; Tildesley, D. J. *Computer Simulation of Liquids*; Oxford Science Publications: Oxford, U.K., 1987.
(21) Frenkel, D.; Smit, B. *Understanding Molecular Simulation*, 2nd ed.; Academic Press: San Diego, CA, 2002.
(22) Sok, R. M.; Berendsen, H. J. C.; van Gunsteren, W. F. *J. Chem. Phys.* **1992**, *96*, 4699.
(23) van der Vegt, N. F. A.; Briels, W. J.; Wessling, M.; Strathmann, H. *J. Chem. Phys.* **1996**, *105*, 8849.
(24) Charati, S. G.; Stern, S. A. *Macromolecules* **1998**, *31*, 5529.
(25) Tamai, Y.; Tanaka, H.; Nakanishi, K. *Macromolecules* **1994**, *27*, 4498.
(26) Fritz, L.; Hofmann, D. *Polymer* **1997**, *38*, 1035.
(27) Frischknecht, A. L.; Curro, J. G. *Macromolecules* **2003**, *36*, 2122.
(28) Sides, S. W.; Curro, J.; Grest, G. S.; Stevens, M. J.; Soddemann, T.; Habenschuss, A.; Londono, J. D. *Macromolecules* **2002**, *35*, 6455.
(29) Sun, H. *J. Phys. Chem. B* **1998**, *102*, 7338.
(30) Smith, J. S.; Borodin, O.; Smith, G. D. *J. Phys. Chem. B* **2004**, *108*, 20340.
(31) Flory, P. J. *Statistical Mechanics of Chain Molecules*; Wiley: New York, 1969.
(32) Nosé, S.; Klein, M. L. *Mol. Phys.* **1983**, *50*, 1055.
(33) Nosé, S. *J. Chem. Phys.* **1984**, *81*, 511.
(34) Nosé, S. *Mol. Phys.* **1984**, *52*, 255.
(35) Gear, C. W. *Numerical Initial Value Problems in Ordinary Differential Equations*; Prentice Hall: Englewood Cliffs, NJ, 1971.
(36) Raptis, V. E.; Economou, I. G.; Theodorou, D. N.; Petrou, J.; Petropoulos, J. H. *Macromolecules* **2004**, *37*, 1102.
(37) Makrodimitri, Z. A.; Raptis, V. E.; Economou, I. G. *J. Phys. Chem. B* **2006**, *110*, 16047.
(38) Details can be found at www.accelrys.com/cerius2/.
(39) Theodorou, D. N.; Boone, T. D.; Dodd, L. R.; Mansfield, K. F. *Macromol. Chem., Theory Simul.* **1993**, *2*, 191.
(40) Widom, B. *J. Chem. Phys.* **1963**, *39*, 2808.
(41) Spyriouni, T.; Economou, I. G.; Theodorou, D. N. *Macromolecules* **1997**, *30*, 4744.
(42) Martin, M. G.; Siepmann, J. I. *J. Phys. Chem. B* **1998**, *102*, 2569.
(43) Cui, S. T.; Siepmann, J. I.; Cochran, H. D.; Cummings, P. T. *Fluid Phase Equilib.* **1998**, *146*, 51.
(44) Cui, S. T.; Cochran, H. D.; Cummings, P. T. *J. Phys. Chem. B* **1999**, *103*, 4485.
(45) Bunn, C. W.; Howells, E. R. *Nature (London)* **1954**, *174*, 549.
(46) Reid, R. C.; Prausnitz, J. M.; Poling, B. E. *The Properties of Gases and Liquids*, 4th ed.; McGraw-Hill: New York, 1987.
(47) Hirschfelder, J. O.; Curtiss, C. F.; Bird, R. B. *Molecular Theory of Gases and Liquids*; Wiley: New York, 1954.
(48) Cheung, P. S. Y.; Powles, J. G. *Mol. Phys.* **1975**, *30*, 921.
(49) Huber, K. P.; Herzberg, G. *Molecular Spectra and Molecular Structure IV. Constants of Diatomic Molecules*; Van Nostrand Reinhold Co.: New York, 1979.
(50) Powles, J. G.; Gubbins, K. E. *Chem. Phys. Lett.* **1976**, *38*, 405.
(51) Theodorou, D. N.; Suter, U. W. *Macromolecules* **1985**, *18*, 1467.
(52) Lee, C. L.; Stern, S. A.; Mark, J. E.; Hoffman, E. Investigation of structure−permeability relationships of silicone polymer membranes. Final Report (October 1982−September 1986), Part I; Gas Research Institute: Chicago, IL, 1982.
(53) Sok, R.M. Ph.D. Thesis, University of Groningen, Groningen, The Netherlands, 1994.
(54) Mattice, W. L.; Suter, U. W. *Conformational Theory of Large Molecules*; Wiley: New York, 1994.
(55) Bahar, I.; Zuniga, I.; Dodge, R.; Mattice, W. L. *Macromolecules* **1991**, *24*, 2986.
(56) Maloney, D. P.; Prausnitz, J. M. *AIChE J.* **1976**, *22*, 74.
(57) van Amerongen, G. J. *J. Appl. Phys.* **1946**, *17*, 972.
(58) van Amerongen, G. J. *Rubber Chem. Technol.* **1964**, *37*, 1065.
(59) Curro, J. G.; Honnell, K. G.; McCoy, J. D. *Macromolecules* **1997**, *30*, 145.

MA062453F